The Molecular Basis for Purine Binding Selectivity in the Bacterial ATP Synthase Subunit

Krah, Alexander; Huber, Roland G.; McMillan, Duncan G.G.; Bond, Peter J.

DOI
10.1002/cbic.202000291

Publication date
2020

Document Version
Final published version

Published in
ChemBioChem

The Molecular Basis for Purine Binding Selectivity in the Bacterial ATP Synthase ε Subunit

Alexander Krah,*[a, b] Roland G. Huber,[a] Duncan G. G. McMillan,[c] and Peter J. Bond*[a, d]

The ε subunit of ATP synthases has been proposed to regulate ATP hydrolysis in bacteria. Prevailing evidence supports the notion that when the ATP concentration falls below a certain threshold, the ε subunit changes its conformation from a non-inhibitory down-state to an extended up-state that then inhibits enzymatic ATP hydrolysis by binding to the catalytic domain. It has been demonstrated that the ε subunit from *Bacillus* PS3 is selective for ATP over other nucleotides, including GTP. In this study, the purine triphosphate selectivity is rationalized by using results from MD simulations and free energy calculations for the R103A/R115A mutant of the ε subunit from *Bacillus* PS3, which binds ATP more strongly than the wild-type protein. Our results are in good agreement with experimental data, and the elucidated molecular basis for selectivity could help to guide the design of novel GTP sensors.

Introduction

ATP synthases convert an electrochemical ion gradient (H^+ or Na^+) across biological membranes into a more stable chemical energy storage unit, adenosine triphosphate (ATP), through an enzymatic reaction involving a dual-motor mechanism.[1] ATP synthases can also catalyse the reverse reaction, in which they release the chemical potential stored in ATP to maintain cellular pH homeostasis or rapidly eject excess Na^+.[2] However, one bacterial ATP synthase is unable to hydrolyse ATP under physiological conditions.[3,4] The reaction is carried out by the soluble F_1 domain, whereas ions are conducted through the membrane-embedded F_o domain concomitant with rotational motion of the proteolipid c subunit ring relative to the stator a subunit. Recent cryo-electron microscopy (cryo-EM) data have provided novel insights into the ion permeation mechanism,[5–7] thus suggesting the existence of two – commonly open – water channels through which ions are translocated. Interestingly, the evolutionarily related V-type ATPase, which has a similar structural morphology but only performs ATP hydrolysis, is also predicted to translocate ions by rotational motion of the c subunit ring. However, cryo-EM[8,9] and simulation[10] data have suggested that these enzymes are able to close one channel in the isolated membrane-embedded V_o domain. Thus, further studies are need to be evaluate this apparent "uncoupling" of ATP hydrolysis from ion translocation.

Although all F-type ATP synthases share a common mechanism to prevent wasteful ATP consumption, namely Mg-ADP inhibition,[11] bacteria and mitochondria have developed diverse secondary mechanisms. In mitochondria, ATP hydrolysis is regulated by the pH-dependent[12] inhibitory protein IF_1.[13] In contrast, most bacterial ATP hydrolysis activity is proposed to be regulated by the ε subunit,[14] which switches its conformation in response to changing ATP concentrations, as shown by biophysical experiments.[15,16] Structural studies have identified an up-state[7,17–19] and a down-state[19] in the F_1 domain of several bacteria. In *Escherichia coli* the up-state is proposed to be inhibitory to ATP hydrolysis and the down-state noninhibitory.[17,19–23] However, studies using an ε subunit mutant incapable of binding ATP across several growth conditions found no difference in growth kinetics, cell yield or survival.[24] Compounding this, the purpose of the ε subunit up- and down-states might be organism-specific; for example, the ε subunit of *Parracoccus denitrificans* ATP synthase has been shown not to regulate ATP hydrolysis *in vitro*.[25] It has been proposed that in α-proteobacteria such as *P. denitrificans*, the ζ subunit has a similar function and mechanism of action to IF_1 in mitochondria,[25] and is also regulated by ATP binding and release, leading to a conformational change in this protein.[26] Equally, it has been counter-claimed that deletion of the ζ subunit has a limited effect on ATP hydrolysis in membranes and no effect on ATP synthesis.[27] Clearly, the field is divided on the different regulatory mechanisms,[28] and close attention needs to be paid to better align microbiological and *in vitro* data. It should be noted that the ε subunit has also been proposed to fulfil other structural and mechanistic roles, such as in ensuring the tight coupling of ATP synthesis and ion translocation,[29,30] accelerating the synthesis and release of ATP from the F_1 domain,[31] or increasing the structural stability of the entire complex through molecular interactions with the membrane-embedded domain.[32]

[a] Dr. A. Krah, Dr. R. G. Huber, Dr. P. J. Bond
Bioinformatics Institute, Agency for Science, Technology and Research (A*STAR)
30 Biopolis Str. #07-01 Matrix, Singapore 138671 (Singapore)
E-mail: kraha@bii.a-star.edu.sg
peterjb@bii.a-star.edu.sg
[b] Dr. A. Krah
Korea Institute for Advanced Study, School of Computational Sciences
85 Hoegiro, Dongdaemun-gu, Seoul, 02455 (Republic of Korea)
[c] Dr. D. G. G. McMillan
Delft University of Technology, Department of Biotechnology
Van der Maasweg 9, Delft 2629HZ (The Netherlands)
[d] Dr. P. J. Bond
National University of Singapore, Department of Biological Sciences
14 Science Drive 4, Singapore 117543 (Singapore)

Supporting information for this article is available on the WWW under https://doi.org/10.1002/cbic.202000291

In vitro studies suggest that the range of ATP concentrations triggering the conformational change of the ε subunit varies from species to species.[15,16,33,34] In line with this, the measured ATP binding affinities of the isolated bacterial ε subunit are 4 μM,[35] 2 mM,[36] and 22 mM[37] in *Bacillus* PS3, *Bacillus subtilis* and *Escherichia coli*, respectively. The K_d for ATP is controlled by the composition of the binding site as initially proposed based on a sequence alignment of *Bacillus* PS3 and *E. coli*,[14] as well as likely allosteric effects.[38] This ATP binding strength can be modified; for example, a R103A/R115A mutant of *Bacillus* PS3 binds ATP three[39] to 100 times more strongly than its WT counterpart ($K_d = 52$ nM),[40] with the precise increase apparently dependent upon the fluorescence dye used to carry out the measurements. The increased affinity of double[41] and single[42] mutants is proposed to arise from an enhanced hydrogen bonding network with ATP compared to the WT protein.[43]

Nucleotides other than ATP do not measurably bind to the WT ε subunit from *Bacillus* PS3.[44] In the case of the *Bacillus* PS3 R103A/R115A double mutant, its affinity for ADP or GTP is two to three orders of magnitude lower than for ATP, with K_d values in the micromolar range.[40] This strong selectivity has also been reported for genetically encoded FRET sensors based on ε subunits engineered to measure ATP concentration in living cells.[45,46] However, at present, the molecular basis for this selectivity is unclear. Although crystallographic analysis reveals important structural information, it typically represents a snapshot of a single state. In contrast, molecular dynamics (MD) simulations provide a means to realistically describe biomolecular motion, and yield insights into the dynamics of proteins, the effects of mutations, and their interactions as a part of complexes. Example applications include investigations of ion binding,[47–49] energetic characterization of protonation states,[48] or the characterization of ligand binding to proteins (including, e.g., protein–ion,[47,49] protein–lipid,[50,51] or protein–inhibitor interactions[52]).

We use MD simulations and free energy calculations to clarify the underlying structural and energetic determinants of purine base (ATP vs. GTP) selectivity in the R103A/R115A mutant of the ε subunit from *Bacillus* PS3. Thus, additional information is obtained regarding the biological mode of action of the ATP synthase ε subunit in a structural context. Furthermore, the framework developed should help in the future design of novel GTP sensors based on this mutant ε subunit, by engineering of additional site-directed mutations. These mutant ε subunits could be merged with fluorescent dyes[45] or fluorescent proteins,[46,53] enabling the GTP concentration to be sensed in real time. These sensors may help to measure in the desired concentration range necessary for *in vivo* cellular conditions. To our knowledge, there is only one fluorescence-based GTP sensor available, and this sensor is not sensitive at physiologically relevant concentrations.[54]

Results & Discussion

GTP binding to the ε subunits from *Bacillus* PS3 and comparison with the ATP binding mode

We derived the initial structure of the R103A/R115A mutant from our recently reported study.[41] This computational study was based on previous simulations of the WT protein[43] using the crystal structure,[37] highlighting the differences in the ATP binding site and the location of the R103A and R115A mutations. It should be mentioned that the physiologically irrelevant R103A/R115A mutant was used, as experimental data are available for this mutant.[40] However, the biologically relevant mechanism of nucleotide binding is expected to be similar in the isolated ε subunit for the WT and mutant. We modelled GTP in the binding site by superimposing the guanosine base onto the adenosine one. Using this initial setup, we aimed to use simulations to identify the GTP binding mode and to assess the stability of binding to the ε subunit from *Bacillus* PS3. We carried out conventional MD simulations for two states: a Mg^{2+} ion was bound either to the GTP:Oα/Oβ or GTP:Oβ/Oγ atoms. A similar strategy previously used for ATP[41,42] revealed that Mg^{2+} is coordinated by ATP:Oα/Oβ, as also shown in a crystal structure of the ε subunit from *Caldalkalibacillus thermarum*;[55] this result was also found for GTP (see the next section).

We observed during MD simulations of the R103A/R115A ε subunit bound to GTP that the nucleoside is bound to D87:O (GTP:N1), E83:Oεx (GTP:O2′), D87:O (GTP:N2), D89:N (GTP:O6) and R92:NHx (GTP:O4′) through hydrogen bonds, and cation-π interactions were also observed with the purine base (Figure 1 and Figure S1 in the Supporting Information). In addition, GTP:Oα is stably coordinated by R126:NHx and additional hydrogen bonds to R122:NHX and R122:Nε can be observed. GTP:Oβ is not stably coordinated by any interaction, but binding and unbinding of arginine residues can be observed. R92:NHx, R92:Nε and R99:NHx stably bind to GTP:Oγ. The probability distributions and the final proposed binding site are shown in Figures 1, 2 and S1. Based on the derived data, a similar binding mode is observed with the phosphate groups for both ATP and GTP.[41] However, binding of the guanosine base to the protein differs; GTP:N1 is a hydrogen bond donor, whereas ATP:N1 is a hydrogen bond acceptor, and GTP:O6 is an acceptor, whereas ATP:N6 is a donor. This is the result of spontaneous rearrangement of key interactions during the simulations, due to the different structure of the base. Instead, additional hydrogen bonds were formed, such as GTP:N1 with D87:O and GTP:N2 with D87:O. The guanosine base remained stably bound, despite the lower experimental affinity of GTP compared to ATP.[40] However, it should be kept in mind that both ligands bind with measurable affinity to the R103A/R115A mutant of the ε subunit (K_d for ATP = 52 nM; K_d for GTP = 53 μM).[40] In addition, based on previous computational observations, the interaction of R126:NHx–GTP:O5′ is weakened with respect to R126:NHx–ATP:O5′.[41] A comparison between the ATP and GTP bound states is shown in Figures 2 and S1.

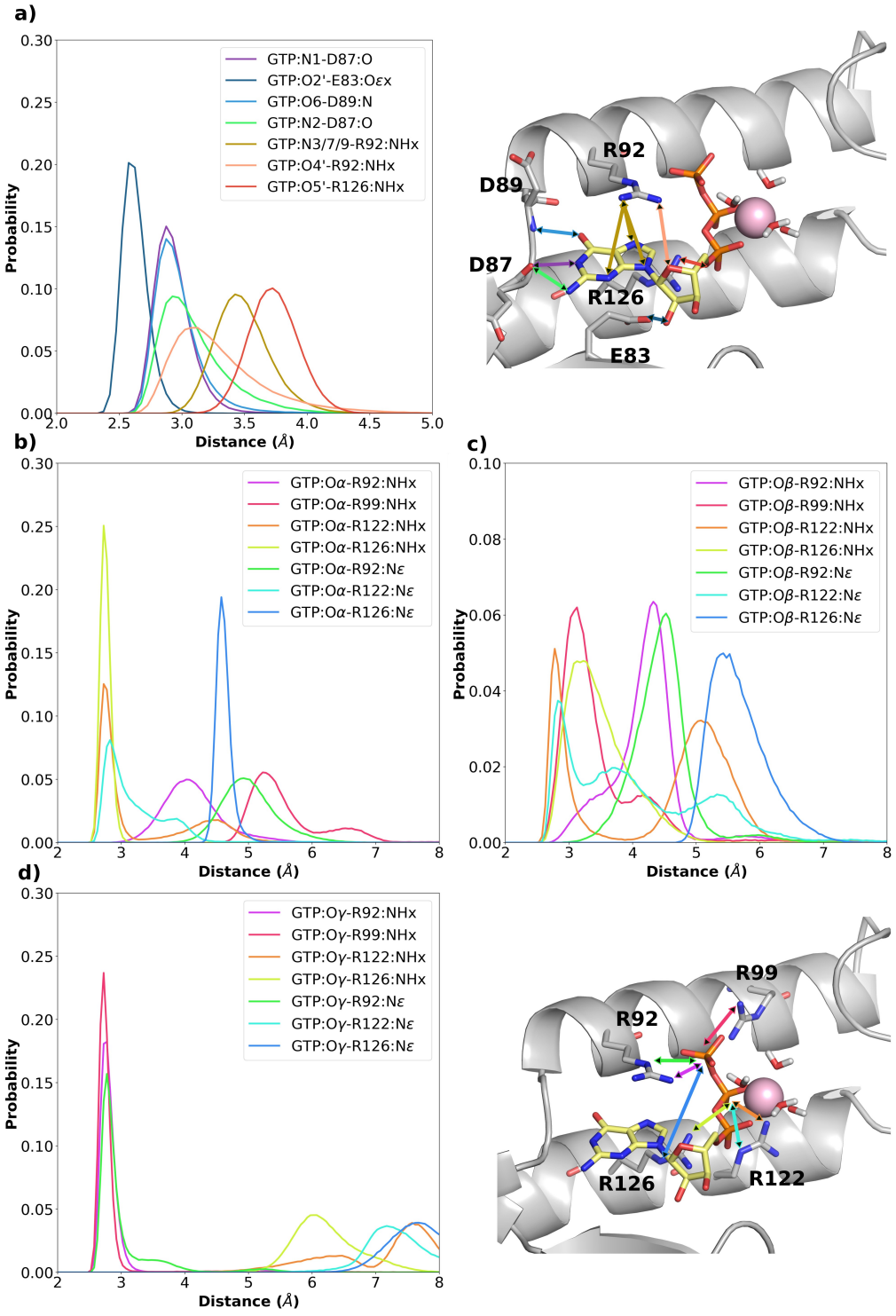

Figure 1. Predicted GTP binding site when Mg^{2+} is bound to GTP:Oα/Oβ in the R103A/R115A ε subunit. Histograms of the interactions of the protein with GTP and graphical representations of these interactions. Sampling was derived from three independent runs, each simulated for 100 ns. Molecular information was visualized by using PyMOL[56]. A LigPlot+[57] sketch of the ATP and GTP binding site is shown in Figure S1. The corresponding data for the system when Mg^{2+} is bound to GTP:Oβ/Oγ instead of GTP:Oα/Oβ is shown in Figure S2. A comparison of the starting model of the binding site versus a representative structure from simulation is shown in Figure S3. In the simulation snapshots, the protein is shown in cartoons format, key residues in CPK-coloured liquorice representation, and the magnesium ion as a van der Waal's sphere.

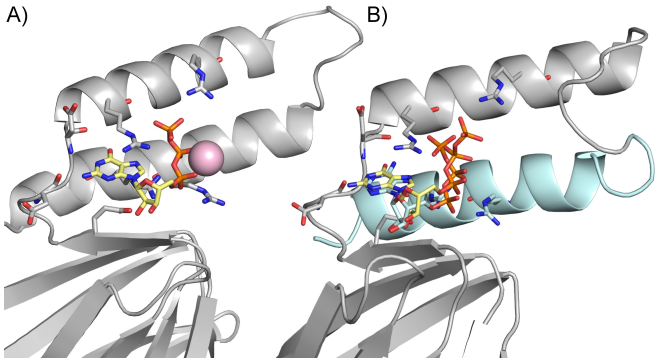

Figure 2. GTP binding site. A) Predicted GTP binding to the R103A/R115A mutant ε subunit from *Bacillus* PS3 based on the distance distributions (Figure 1) and the energetic analysis. B) Comparison of ATP and GTP binding. The Mg^{2+} ion is omitted for clarity. The second helix (residues 112–132), also analysed in the Espinosa approach, is highlighted in cyan.

Table 1. Energetic analysis of ion coordination and nucleotide binding. A) The number of hydrogen bonds of the protein with GTP and of the second helix (residues 112–132) with the rest of the protein, as graphically represented in Figure 2. B) The enthalpic contributions [kcal/mol] estimated by using the method of Espinosa et al.[58] The data were calculated when GTP was bound to the R103A/R115A mutant of the ε subunit from *Bacillus* PS3, and the ion was bound either to GTP:Oα/Oβ or GTP:Oβ/Oγ. The data are also compared to results for ATP:Oα/Oβ based on our previous work.[41] All data here were derived from simulations of three 100 ns replicas per system.

	GTP:Oα/Oβ	GTP:Oβ/Oγ	ATP:Oα/Oβ[41]
A) Number of hydrogen bonds			
protein–nucleotide	12.0 ± 0.3	9.7 ± 1.1	10.4 ± 0.6
2nd helix	4.2 ± 0.2	4.5 ± 0.9	4.1 ± 0.2
total	16.2 ± 0.4	14.1 ± 1.6	14.4 ± 0.5
B) Enthalpic contributions [kcal/mol]			
protein–nucleotide	−85.0 ± 1.4	−67.8 ± 4.4	−73.4 ± 2.1
2nd helix	−28.6 ± 2.1	−30.8 ± 4.9	−26.4 ± 1.5
whole contribution	−113.6 ± 3.5	−98.6 ± 9.2	−99.8 ± 1.8

To further rationalize the experimentally measured affinities, and to test our predictions, we next investigated the energetic contribution of ligand binding to the R103A/R115A mutant ε subunit from *Bacillus* PS3.

Ion binding and enthalpic contributions of GTP interaction with the R103A/R115A mutant ε subunit

We recently predicted that a Mg^{2+} ion is coordinated by ATP:Oα/Oβ, rather than to ATP:Oβ/Oγ, when ATP is bound to the ε subunit from *Bacillus* PS3.[41–43] This has also now been substantiated in a crystal structure of the ε subunit from *C. thermarum*,[55] providing solid evidence that MD simulations are valid for this type of analysis. To test if the Mg^{2+} ion is more likely coordinated by GTP:Oα/Oβ or GTP:Oβ/Oγ, we performed an enthalpic analysis introduced by Espinosa *et al.*[58] (see the Experimental Section for details). This allows us to predict the likely ion position when complexed with ATP bound to the R103A/R115A mutant.[41] Based on the energetic contributions of GTP-protein interactions and interactions of the second helix (residues 112–132; Figure 2)) along with the rest of the protein, we conclude that the Mg^{2+} ion is likely coordinated to ATP:Oα/Oβ in both the R103A/R115A mutant[41] and the WT protein.[43] The large standard deviations for the GTP:Oβ/Oγ state indicate that it is not a very stable interaction (Table 1).

Table 2. Contributions of structural components to nucleotide binding to the protein. A) The number of hydrogen bonds. B) The results of the energetic analysis (enthalpic contributions [kcal/mol] based on the method of Espinosa et al.[58]). The energetic analysis is carried out for the ion when bound to GTP:Oα/Oβ or GTP:Oβ/Oγ. In addition, we reanalysed our previous work for comparison with the ATP bound state (ATP:Oα/Oβ)[41]. All data here were derived from simulations of three 100 ns replicas per system.

	GTP:Oα/Oβ	GTP:Oβ/Oγ	ATP:Oα/Oβ
A) Number of hydrogen bonds			
base	2.6 ± 0.03	2.6 ± 0.07	1.9 ± 0.01
sugar	1.6 ± 0.05	1.8 ± 0.1	1.2 ± 0.04
phosphate	7.8 ± 0.2	5.4 ± 0.97	7.2 ± 0.6
B) Enthalpic contributions [kcal/mol]			
base	−12.7 ± 0.1	−12.8 ± 0.3	−7.7 ± 0.1
sugar	−17.5 ± 0.3	−18.2 ± 0.9	−15.4 ± 0.5
phosphate	−54.8 ± 1.1	−36.8 ± 3.9	−50.5 ± 2.3

To understand the individual contributions of the different functional segments of the nucleotide to the enthalpic part of protein binding, we split the energies into base, sugar, and phosphate components. Surprisingly, the enthalpic contribution of all structural elements was energetically more favourable for GTP than for ATP (Table 2). However, it should be noted that the guanosine base has an increased number of potential hydrogen bond donors and acceptors compared to ATP. Thus, a rearrangement of GTP in the binding site (Figures 1 and 2) allows an increased number of interactions compared to ATP. In addition, the rearrangement of the guanine base in the binding site allows for a higher enthalpic contribution of the sugar and phosphate groups. However, the binding free energy difference estimated using this method[58] does not account for entropic contributions, which may account for the apparent increase in affinity for GTP over ATP.

Energetic insights into the ATP vs. GTP selectivity based on free energy calculations

To account for both the enthalpic and entropic contributions to protein–ligand binding free energy, we next employed thermodynamic integration (TI) calculations to rationalize ATP versus GTP selectivity. We calculated the free energy of transforming ATP to GTP in both water and when bound to the R103A/R115A mutant, for comparison with the available experimental data.[40] The free energy difference could be calculated by using a thermodynamic cycle (Figure 3). Our calculations accurately reproduced the experimental results, with a $\Delta\Delta G$ of ~4 kcal/mol for ATP selectivity over GTP. We thus conclude that our bound model of GTP to the R103A/R115A mutant derived from conventional MD simulations is accurate. Furthermore, we show that the nucleotide binding is mainly governed by entropy, since the enthalpy of GTP binding is apparently more favour-

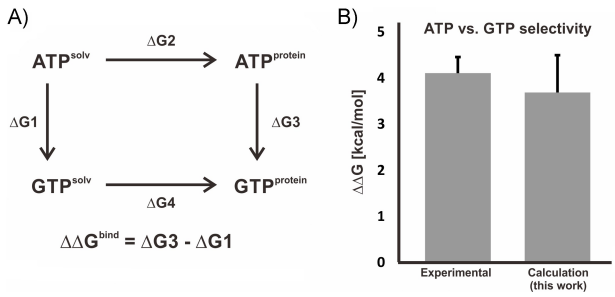

Figure 3. ATP vs. GTP selectivity. A) The thermodynamic cycle. B) Data based on experiments[40] or the theoretical calculations reported in the present work.

able (Tables 1 and 2). Our results are also in agreement with previous calculations based on the solvation free energies of 9-methylguanosine and 9-methyladenine[59], indicating there should be a significantly higher solvation free energy for GTP in comparison with ATP.

Conclusions

In this study, we clarified the molecular and energetic basis for purine (ATP vs. GTP) selectivity in an ε subunit from a bacterial F-type ATP synthase. First, we predicted the binding mode of GTP to the R103A/R115A ε subunit mutant from *Bacillus* PS3. Secondly, based on the dynamics derived from conventional MD simulations, we calculated the enthalpic properties of GTP binding. Lastly, we used rigorous free energy calculations to accurately assess the energetics of purine selectivity including entropic effects. Collectively, this demonstrated that the binding energetics of our models accurately reflect experimental findings, thus supporting our structural hypothesis. The information obtained in this study provides a strong molecular rationale: 1) to explain nucleotide selectivity in a biologically important bacterial protein; and 2) to drive the design of novel nucleotide sensors based on bacterial F-ATP synthase ε subunits.

Experimental Section

Conventional MD simulations were performed by using the GROMACS program suite[60] and the AMBER-ILDN force field.[61-64] The R103A/R115A mutant ε subunit from *Bacillus* PS3 was assessed in the GTP bound state following the framework described in our previous studies.[38,41,43] In a first set of simulations, the Mg^{2+} ion was coordinated to the ATP:Oα/Oβ atoms, and in a second set, the Mg^{2+} ion was coordinated by the ATP:Oβ/Oγ atoms. These simulations were each carried out for 100 ns in triplicate. The free energy difference of the ATP to GTP transformation was calculated using theTI approach. For the transition of ATP to GTP, we used 32 λ windows, as previously described; λ = {0, 0.05, 0.1, 0.15, 0.2, 0.25, 0.3, 0.35, 0.4, 0.45, 0.5, 0.54, 0.58, 0.62, 0.66, 0.7, 0.73, 0.76, 0.79, 0.82, 0.85, 0.87, 0.89, 0.91, 0.93, 0.95, 0.96, 0.97, 0.98, 0.99, 0.995, 1}.[48] Each window was simulated for 5 ns and the first 500 ps period of each window was discarded as equilibration time. We calculated the relative free energy of this transformation (ATP→GTP) using two sets of simulations; specifically, the transformation of the ligand was carried out when 1) bound to the R103A/R115A mutant, and 2) in bulk solvent. We then used a thermodynamic cycle to obtain the ATP to GTP binding free energy change of the double mutant with respect to the solvated state; this approach allows us to assume the same energetic contributions for breaking/building covalent interactions, as discussed previously.[65] Results obtained from the TI simulations were analysed using the Bennett acceptance ratio (BAR) method.[66] All TI simulations were carried out in triplicate.

To analyse enthalpic contributions and to elucidate whether the Mg^{2+} ion is more likely bound to GTP:Oα/Oβ or GTP:Oβ/Oγ, we used an energetic analysis method to assess the protein–ligand hydrogen bond network, as described by Espinosa et al.[58] In addition, the protein–protein hydrogen bond network within the second α-helical C-terminal domain (residues 112–133) was analysed by using the same approach. For this, we used a cut-off distance of 2.7 Å from the acceptor atom to the donor hydrogen atom and a cut-off of 30° for the angle between donor hydrogen atom, donor heavy atom, and acceptor atom. This analysis calculates the enthalpic contribution for ligand binding to a protein, based on the estimation of the energy of the hydrogen bonding network. The strength of a hydrogen bond is calculated as follows:

$$E_{HB} = -\frac{50}{2} \times 10^3 \times e^{(-3.6\,d(H-O))}\ [kJ/mol]$$

where E_{HB} refers to the enthalpic energy of the hydrogen bond and d(H–O) denotes the distance between the donor hydrogen and the acceptor atom in Å.[58] Entropic contributions are not taken into account in this method. The first 10 ns of each simulation were discarded from this analysis for equilibration purposes.

Acknowledgements

*AK would like to thank the KIAS Center for Advanced Computation for providing computing resources for the initial stage of this work. Additional computational resources were provided by the National Supercomputing Centre, Singapore (https://www.nscc.sg). We thank BII (A*STAR) for funding. This work was supported by a TU Delft StartUP fund (to DGGM).*

Conflict of Interest

The authors declare no conflict of interest.

Keywords: ATP synthase · *Bacillus* PS3 · epsilon subunit · ligand selectivity · molecular dynamics simulations

[1] M. Diez, B. Zimmermann, M. Börsch, M. König, E. Schweinberger, S. Steigmiller, R. Reuter, S. Felekyan, V. Kudryavtsev, C. A. M. Seidel, et al., *Nat. Struct. Mol. Biol.* **2004**, *11*, 135–41.
[2] H. Noji, R. Yasuda, M. Yoshida, K. Kinosita, *Nature* **1997**, *386*, 299–302.
[3] D. G. G. McMillan, S. Keis, P. Dimroth, G. M. Cook, *J. Biol. Chem.* **2007**, *282*, 17395–17404.

[4] D. G. G. McMillan, R. Watanabe, H. Ueno, G. M. Cook, H. Noji, *J. Biol. Chem.* **2016**, *291*, 23965–23977.
[5] M. Allegretti, N. Klusch, D. J. Mills, J. Vonck, W. Kühlbrandt, K. M. Davies, *Nature* **2015**, *521*, 237–240.
[6] A. Hahn, J. Vonck, D. J. Mills, T. Meier, W. Kühlbrandt, *Science* **2018**, *360*, eaat4318.
[7] H. Guo, T. Suzuki, J. L. Rubinstein, *eLife* **2019**, *8*, e43128.
[8] M. T. Mazhab-Jafari, A. Rohou, C. Schmidt, S. A. Bueler, S. Benlekbir, C. V. Robinson, J. L. Rubinstein, *Nature* **2016**, *539*, 118–122.
[9] S.-H. Roh, N. J. Stam, C. F. Hryc, S. Couoh-Cardel, G. Pintilie, W. Chiu, S. Wilkens, *Mol. Cell* **2018**, *69*, 993–1004.e3.
[10] A. Krah, J. K. Marzinek, P. J. Bond, *Biochim. Biophys. Acta Biomembr.* **2019**, *1861*, 1004–1010.
[11] Y. Hirono-Hara, H. Noji, M. Nishiura, E. Muneyuki, K. Y. Hara, R. Yasuda, K. Kinosita, M. Yoshida, *Proc. Natl. Acad. Sci. USA* **2001**, *98*, 13649–54.
[12] E. Cabezon, P. J. G. Butler, M. J. Runswick, J. E. Walker, *J. Biol. Chem.* **2000**, *275*, 25460–25464.
[13] M. E. Pullman, G. C. Monroy, *J. Biol. Chem.* **1963**, *238*, 3762–9.
[14] A. Krah, M. Zarco-Zavala, D. G. G. McMillan, *Open Biol.* **2018**, *8*, 170275.
[15] B. A. Feniouk, T. Suzuki, M. Yoshida, *J. Biol. Chem.* **2007**, *282*, 764–72.
[16] B. A. Feniouk, Y. Kato-Yamada, M. Yoshida, T. Suzuki, *Biophys. J.* **2010**, *98*, 434–442.
[17] G. Cingolani, T. M. Duncan, *Nat. Struct. Mol. Biol.* **2011**, *18*, 701–7.
[18] Y. Shirakihara, A. Shiratori, H. Tanikawa, M. Nakasako, M. Yoshida, T. Suzuki, *FEBS J.* **2015**, *282*, 2895–913.
[19] M. Sobti, R. Ishmukhametov, J. C. Bouwer, A. Ayer, C. Suarna, N. J. Smith, M. Christie, R. Stocker, T. M. Duncan, A. G. Stewart, *eLife* **2019**, *8*, e43864 .
[20] M. Nakanishi-Matsui, S. Kashiwagi, H. Hosokawa, D. J. Cipriano, S. D. Dunn, Y. Wada, M. Futai, *J. Biol. Chem.* **2006**, *281*, 4126–31.
[21] S. D. Bockenhauer, T. M. Duncan, W. E. Moerner, M. Börsch, *Proc. SPIE*, **2014**, *8950*, 89500H.
[22] M. Sobti, C. Smits, A. S. Wong, R. Ishmukhametov, D. Stock, S. Sandin, A. G. Stewart, *eLife* **2016**, *5*, e21598.
[23] M. Nakanishi-Matsui, M. Sekiya, S. Yano, M. Futai, *J. Biol. Chem.* **2014**, *289*, 30822–30831.
[24] N. Taniguchi, T. Suzuki, M. Berney, M. Yoshida, G. M. Cook, *J. Bacteriol.* **2011**, *193*, 2046–2052.
[25] E. Morales-Ríos, F. de la Rosa-Morales, G. Mendoza-Hernández, J. S. Rodríguez-Zavala, H. Celis, M. Zarco-Zavala, J. J. García-Trejo, *FASEB J.* **2010**, *24*, 599–608.
[26] M. Zarco-Zavala, E. Morales-Ríos, G. Mendoza-Hernández, L. Ramírez-Silva, G. Pérez-Hernández, J. J. García-Trejo, *FASEB J.* **2014**, *28*, 2146–57.
[27] F. Varghese, J. N. Blaza, A. J. Y. Jones, O. D. Jarman, J. Hirst, *Open Biol.* **2018**, *8*, 170206.
[28] A. Krah, *Prog. Biophys. Mol. Biol.* **2015**, *119*, 94–102.
[29] F. Kadoya, S. Kato, K. Watanabe, Y. Kato-Yamada, *Biochem. J.* **2011**, *437*, 135–40.
[30] G. Akanuma, T. Tagana, M. Sawada, S. Suzuki, T. Shimada, K. Tanaka, F. Kawamura, Y. Kato-Yamada, *MicrobiologyOpen* **2019**, e815.
[31] R. Watanabe, M. Genda, Y. Kato-Yamada, H. Noji, *Biophys. J.* **2018**, *114*, 178–187.
[32] D. Pogoryelov, Y. Nikolaev, U. Schlattner, K. Pervushin, P. Dimroth, T. Meier, *FEBS J.* **2008**, *275*, 4850–4862.
[33] S. P. Tsunoda, A. J. Rodgers, R. Aggeler, M. C. Wilce, M. Yoshida, R. A. Capaldi, *Proc. Natl. Acad. Sci. USA* **2001**, *98*, 6560–4.
[34] T. Suzuki, T. Murakami, R. Iino, J. Suzuki, S. Ono, Y. Shirakihara, M. Yoshida, *J. Biol. Chem.* **2003**, *278*, 46840–6.
[35] S. Kato, M. Yoshida, Y. Kato-Yamada, *J. Biol. Chem.* **2007**, *282*, 37618–37623.
[36] Y. Kato-Yamada, *FEBS Lett.* **2005**, *579*, 6875–6878.
[37] H. Yagi, N. Kajiwara, H. Tanaka, T. Tsukihara, Y. Kato-Yamada, M. Yoshida, H. Akutsu, *Proc. Natl. Acad. Sci. USA* **2007**, *104*, 11233–11238.
[38] A. Krah, S. Takada, *Biochim. Biophys. Acta Bioenerg.* **2015**, *1847*, 1101–1112.
[39] M. Fujiwara, Y. Kato-Yamada, *Biochem. Biophys. Reports* **2020**, *21*, 100725.
[40] Y. Kato-Yamada, *Biochem. Biophys. Res. Commun.* **2016**, *469*, 1129–1132.
[41] A. Krah, Y. Kato-Yamada, S. Takada, *PLoS One* **2017**, *12*, e0177907.
[42] A. Krah, P. J. Bond, *PeerJ* **2018**, *6*, e5505.
[43] A. Krah, S. Takada, *Biochim. Biophys. Acta Bioenerg.* **2016**, *1857*, 332–340.
[44] Y. Kato-Yamada, M. Yoshida, *J. Biol. Chem.* **2003**, *278*, 36013–36016.
[45] H. Imamura, K. P. H. Nhat, H. Togawa, K. Saito, R. Iino, Y. Kato-Yamada, T. Nagai, H. Noji, *Proc. Natl. Acad. Sci. USA* **2009**, *106*, 15651–6.
[46] H. Yaginuma, S. Kawai, K. V. Tabata, K. Tomiyama, A. Kakizuka, T. Komatsuzaki, H. Noji, H. Imamura, *Sci. Rep.* **2014**, *4*, 6522.
[47] T. Meier, A. Krah, P. J. Bond, D. Pogoryelov, K. Diederichs, J. D. Faraldo-Gómez, *J. Mol. Biol.* **2009**, *391*, 498–507.
[48] A. Krah, U. Zachariae, *Phys. Biol.* **2017**, *14*, 045009.
[49] A. Krah, R. G. Huber, U. Zachariae, P. J. Bond, *Biochim. Biophys. Acta Biomembr.* **2020**, *1862*, 183137.
[50] J. K. Marzinek, D. A. Holdbrook, R. G. Huber, C. Verma, P. J. Bond, *Structure* **2016**, *24*, 1410–1420.
[51] J. Yeow, K. W. Tan, D. A. Holdbrook, Z. S. Chong, J. K. Marzinek, P. J. Bond, S. S. Chng, *J. Biol. Chem.* **2018**, *293*, 11325–11340.
[52] S. Re, H. Oshima, K. Kasahara, M. Kamiya, Y. Sugita, *Proc. Natl. Acad. Sci. USA* **2019**, *116*, 18404–18409.
[53] T. Yoshida, A. Kakizuka, H. Imamura, *Sci. Rep.* **2016**, *6*, 39618.
[54] A. Bianchi-Smiraglia, M. S. Rana, C. E. Foley, L. M. Paul, B. C. Lipchick, S. Moparthy, K. Moparthy, E. E. Fink, A. Bagati, E. Hurley, et al., *Nat. Methods* **2017**, *14*, 1003–1009.
[55] S. A. Ferguson, G. M. Cook, M. G. Montgomery, A. G. W. Leslie, J. E. Walker, *Proc. Natl. Acad. Sci. USA* **2016**, *113*, 10860–5.
[56] Schrodinger LLC, **2015**.
[57] R. A. Laskowski, M. B. Swindells, *J. Chem. Inf. Model.* **2011**, *51*, 2778–2786.
[58] E. Espinosa, E. Molins, C. Lecomte, *Chem. Phys. Lett.* **1998**, *285*, 170–173.
[59] M. G. Wolf, G. Groenhof, *J. Comput. Chem.* **2012**, *33*, 2225–2232.
[60] M. J. Abraham, T. Murtola, R. Schulz, S. Páll, J. C. Smith, B. Hess, E. Lindahl, *SoftwareX* **2015**, *1–2*, 19–25.
[61] W. D. Cornell, P. Cieplak, C. I. Bayly, I. R. Gould, K. M. Merz, D. M. Ferguson, D. C. Spellmeyer, T. Fox, J. W. Caldwell, P. A. Kollman, *J. Am. Chem. Soc.* **1995**, *117*, 5179–5197.
[62] K. L. Meagher, L. T. Redman, H. A. Carlson, *J. Comput. Chem.* **2003**, *24*, 1016–1025.
[63] V. Hornak, R. Abel, A. Okur, B. Strockbine, A. Roitberg, C. Simmerling, *Proteins Struct. Funct. Bioinf.* **2006**, *65*, 712–725.
[64] K. Lindorff-Larsen, S. Piana, K. Palmo, P. Maragakis, J. L. Klepeis, R. O. Dror, D. E. Shaw, *Proteins Struct. Funct. Bioinf.* **2010**, *78*, 1950–1958.
[65] A. Krah, D. Pogoryelov, J. D. Langer, P. J. Bond, T. Meier, J. D. Faraldo-Gómez, *Biochim. Biophys. Acta Bioenerg.* **2010**, *1797*, 763–772.
[66] C. H. Bennett, *J. Comput. Phys.* **1976**, *22*, 245–268.

Manuscript received: May 11, 2020
Revised manuscript received: June 30, 2020
Accepted manuscript online: June 30, 2020
Version of record online: ■■, ■■■

FULL PAPERS

The ups and downs of purine binding: Nucleotide binding to the bacterial ε subunit causes a conformational change from the up- to the down-state. In this study, we clarify the structural and energetic basis of purine binding and the purine selectivity of the ε subunit from *Bacillus* PS3.